Iterative Scheme for the Darcy-Forchheimer Problem with Pressure Boundary Condition

RIM AL DBAISSY[1], TONI SAYAH[2]

[1]Faculty of engineering (ESIB), Saint Joseph University of Beirut,
LEBANON

[2]Laboratoire de Mathématiques et Applications, URMM, CAR,
Faculté des Sciences, Université Saint-Joseph de Beyrouth,
B.P 11-514 Riad El Solh, Beyrouth 1107 2050,
LEBANON

Abstract: This paper addresses the Darcy-Forchheimer problem with pressure boundary conditions. We employ finite element methods to discretize the system and introduce an iterative scheme to solve the resulting nonlinear discrete problem. The well-posedness and convergence of this iterative approach are then demonstrated. Finally, we present several numerical experiments to validate the proposed numerical schemes.

Key-Words: Darcy-Forchheimer problem, Finite element method, Iterative scheme, *a priori* error estimate.

Received: May 29, 2024. Revised: September 11, 2024. Accepted: November 13, 2024. Published: December 31, 2024.

1 Introduction

Darcy's law describes the creeping flow of Newtonian fluids in porous media. It establishes a linear relationship between the velocity of creeping flow and the pressure gradient, as expressed by the equation

$$\frac{\mu}{\rho}K^{-1}\mathbf{u} + \nabla p = \mathbf{f},$$

where $\mathbf{u}$ represents the velocity, p represents the pressure, and the parameters ρ and μ represent the fluid density and its viscosity.
A theoretical derivation of Darcy's law can be found in [1], [2]. However, when conducting flow experiments in porous media with nonuniform porosity and higher velocities, [3], observed that Darcy's law becomes insufficient. To address this limitation, Forchheimer introduced a modified equation, which is nonlinear in nature:

$$\frac{\mu}{\rho}K^{-1}\mathbf{u} + \frac{\beta}{\rho}|\mathbf{u}|\mathbf{u} + \nabla p = \mathbf{f}. \tag{1}$$

Here, $|.|$ denotes the Euclidean norm, and $|\mathbf{u}|^2 = \mathbf{u}\cdot\mathbf{u}$. The parameter β represents the fluid dynamic viscosity and is also referred to as the Forchheimer number when it is a positive scalar constant. K represents the permeability tensor.
A theoretical derivation of Forchheimer's law can be found in [4].

A mixed element for Forchheimer equation (1), also known as Darcy-Forchheimer equation, completed by a non-homogeneous boundary condition on the normal component of the velocity was introduced by [5]. Their work established the existence and uniqueness of the corresponding weak solution. At the discrete level, Girault and Wheeler approximated the velocity using piecewise constants and the pressure using the Crouzeix-Raviart element. To solve the resulting system of nonlinear equations arising from finite element discretization, they proposed an alternating directions iterative method. Their research encompasses the convergence analysis of both the iterative algorithm and the mixed element scheme. Additionally, they provided an error estimate for the mixed element scheme. The study, [6], carried out numerical tests of the methods studied in [5], to corroborate the results presented there. Furthermore, they introduced another mixed finite element space, which yields smoother pressure approximations compared to the space proposed in [5]. The study, [7], undertook a theoretical study of this mixed finite element space as proposed in [6]. Their work demonstrated the existence and uniqueness of discrete solutions, convergence, and error estimates. The study, [8] derived *a posteriori* error estimates for the Darcy-Forchheimer problem introduced in [5], [7]. Furthermore, their work in [9] extended their investigation to include the coupling of the Darcy-Forchheimer problem with the convection-diffusion-reaction equation. They showed existence and conditional uniqueness of the solution, disctretized it by using the finite element method and establish optimal *a priori* and *a posterior* error estimates.

In a different approach, the authors in [10], considered Equation (1) with boundary conditions on pressure and introduced mixed element approximations, including the Raviart-Thomas mixed element and the Brezzi-Douglas-Marini mixed element. They established the existence and uniqueness of weak solutions and provided corresponding error estimates. Additionally, they introduced an iterative algorithm but did not extensively investigate its convergence. Their work was complemented by numerical tests to validate the proposed methods.

Several recent works have focused on the Darcy-Forccheimer equation and its practical applications; we refer to [11], [12], [13], [14], [15], [16], [17], for theoretical and numerical investigations and to [18], [19], [20], [21], [22], [23], for practical applications.

In this paper, we consider the problem introduced in [10], and recall the corresponding discrete scheme. We subsequently propose a discrete iterative scheme and demonstrate its convergence. Finally, we present numerical simulations to validate our findings.
Let Ω be a bounded subset of $\mathbb{R}^d$ ($d = 2, 3$) with Lipschitz continuous boundary $\Gamma = \partial\Omega$. We consider the Darcy-Forchheimer equation (1) with the divergence constraint

$$\operatorname{div} \mathbf{u} = b \quad \text{in} \quad \Omega, \tag{2}$$

and the boundary condition

$$p = 0 \quad \text{on} \quad \partial\Omega. \tag{3}$$

We assume that the tensor K appearing in (1) is uniformly positive definite and bounded, satisfying:

$$0 < K_m \, \mathbf{x} \cdot \mathbf{x} \leq (K^{-1}(\mathbf{x})\mathbf{x}) \cdot \mathbf{x} \leq K_M \, \mathbf{x} \cdot \mathbf{x}. \tag{4}$$

where K_m and K_M are two positive real numbers.
It's worth noting that K_m could be very close to zero, and K_M could be very large. Although the homogeneous boundary condition (3) can be easily extended to the non-homogeneous case ($p = g_p$ on $\partial\Omega$), we use (3) for simplicity.

We denote by Problem (P) the system of equations (1), (2) and (3).
The structure of this paper is as follows:

- Section 2 describes the problem and the weak formulation.
- Section 3 delves into the discretization process and explores the convergence of the proposed iterative scheme.
- Section 4 presents the results of our numerical simulations.

2 Notations and Weak Formulations

In order to introduce the variational formulations, we recall some classical Sobolev spaces and their properties.

Let $\alpha = (\alpha_1, \alpha_2, \dots \alpha_d)$ be a d-uple of non negative integers, set $|\alpha| = \sum_{i=1}^{d} \alpha_i$, and define the partial derivative ∂^α by

$$\partial^\alpha = \frac{\partial^{|\alpha|}}{\partial x_1^{\alpha_1} \partial x_2^{\alpha_2} \dots \partial x_d^{\alpha_d}}.$$

Then, for any positive integer m and number $q \geq 1$, we recall the classical Sobolev space

$$W^{m,q}(\Omega) = \{v \in L^q(\Omega);\, \forall\, |\alpha| \leq m,\ \partial^\alpha v \in L^q(\Omega)\}, \tag{5}$$

equipped with the seminorm

$$|v|_{W^{m,q}(\Omega)} = \Big\{ \sum_{|\alpha|=m} \int_\Omega |\partial^\alpha v|^q \, d\mathbf{x} \Big\}^{\frac{1}{q}} \tag{6}$$

and the norm

$$\|v\|_{W^{m,q}(\Omega)} = \Big\{ \sum_{0 \leq k \leq m} |v|^q_{W^{k,q}(\Omega)} \Big\}^{\frac{1}{q}}. \tag{7}$$

When $q = 2$, this space is the Hilbert space $H^m(\Omega)$. In particular, the scalar product of $L^2(\Omega)$ is denoted by $(.,.)$.
The definitions of these spaces are extended straightforwardly to vectors, using the same notation, but with the following modification for the norms in the non-Hilbert case. Let $\mathbf{v}$ be a vector valued function and we define the norm as follows:

$$\|\mathbf{v}\|_{L^q(\Omega)} = \Big(\int_\Omega |\mathbf{v}|^q \, d\mathbf{x} \Big)^{\frac{1}{q}}, \tag{8}$$

where $|.|$ denotes the Euclidean vector norm.

We recall the following standard space

$$H(\operatorname{div}, \Omega) = \{\mathbf{v} \in L^2(\Omega)^d;\, \operatorname{div}(\mathbf{v}) \in L^2(\Omega)\}, \tag{9}$$

equipped with the norm

$$\|\mathbf{v}\|^2_{H(\operatorname{div},\Omega)} = \|\mathbf{v}\|^2_{L^2(\Omega)} + \|\operatorname{div}(\mathbf{v})\|^2_{L^2(\Omega)}. \tag{10}$$

Let us now introduce the following technical lemma:

Lemma 2.1. *For all $x, y \in \mathbb{R}$ and $q \in \mathbb{R}^+$, the following bound holds:*

$$(|x|^q x - |y|^q y)(x - y) \geq 0.$$

2.1 Variational Formulation

For all the properties and details of the weak formulation corresponding to Problem (P) presented in this section, we refer to [10]. Let us introduce the spaces $M = L^2(\Omega)$ and

$$X = \{\mathbf{v} \in L^3(\Omega)^d; \mathrm{div}(\mathbf{v}) \in L^2(\Omega)\},$$

equipped with the norm

$$||\mathbf{v}||_X = ||\mathbf{v}||_{L^3(\Omega)} + ||\,\mathrm{div}(\mathbf{v})||_{L^2(\Omega)}.$$

The spaces X and M satisfy the following inf-sup condition: there exists a positive constant γ such that

$$\inf_{q\in M} \sup_{\mathbf{v}\in X} \frac{\displaystyle\int_\Omega q \,\mathrm{div}(\mathbf{v})\, d\mathbf{x}}{||q||_M ||\mathbf{v}||_X} \geq \gamma.$$

In this case, we assume $\mathbf{f} = \nabla Z \in L^2(\Omega)^d$ the gradient of the depth function $Z \in H^1(\Omega)$ and $b \in L^2(\Omega)$ (see, [10], for details).

In order to write the variational formulation associated to Problem (P), we introduce the mapping $\mathbf{v} \longrightarrow \mathcal{A}(\mathbf{v})$ defined by:

$$\begin{array}{llll} \mathcal{A}: & L^3(\Omega)^d & \mapsto & L^{\frac{3}{2}}(\Omega)^d \\ & \mathbf{v} & \mapsto & \mathcal{A}(\mathbf{v}) = \dfrac{\mu}{\rho} K^{-1}\mathbf{v} + \dfrac{\beta}{\rho}|\mathbf{v}|\mathbf{v}. \end{array}$$

We refer to [5], (page 170), and [24], (Lemma 3), for the following properties of $\mathcal{A}$.

Property 2.2. *We have the following monotonicity properties:*

1. *for all* $\mathbf{v} \in L^3(\Omega)^d$,
$$\frac{\mu}{\rho}\int_\Omega K^{-1}\mathbf{v}\cdot\mathbf{v}\, d\mathbf{x} \geq \frac{\mu K_m}{\rho} \|\mathbf{v}\|^2_{L^2(\Omega)} \tag{11}$$
2. *for all* $\mathbf{v}, \mathbf{w} \in L^3(\Omega)^d$,
$$\frac{\beta}{\rho}\int_\Omega (|\mathbf{v}|\mathbf{v} - |\mathbf{w}|\mathbf{w})(\mathbf{v}-\mathbf{w})\, d\mathbf{x} \geq c_m \|\mathbf{v}-\mathbf{w}\|^3_{L^3(\Omega)}. \tag{12}$$
where c_m is a strictly positive constant depending on $|\Omega|$.

Problem (P) is equivalent to the following variational formulation: Find $(\mathbf{u}, p) \in X \times M$ such that

$$\left\{\begin{array}{l} \forall \mathbf{v} \in X, \quad \displaystyle\int_\Omega \mathcal{A}(\mathbf{u})\cdot\mathbf{v}\, d\mathbf{x} - \int_\Omega p \,\mathrm{div}(\mathbf{v})\, d\mathbf{x} \\ \qquad\qquad = \displaystyle\int_\Omega \mathbf{f}\cdot\mathbf{v}\, d\mathbf{x}, \\ \forall q \in M, \quad \displaystyle\int_\Omega q\,\mathrm{div}(\mathbf{u})\, d\mathbf{x} = \int_\Omega b\, q\, d\mathbf{x}. \end{array}\right. \tag{13}$$

As established in [10], Problem (P) is equivalent to (13), and it possesses a unique solution in $(\mathbf{u}, p) \in X \times M$, satisfying the following relations:

$$\begin{aligned} &||\mathbf{u}||^2_{L^2(\Omega)} + ||\mathbf{u}||^3_{L^3(\Omega)} + ||\,\mathrm{div}(\mathbf{u})||^2_{L^2(\Omega)} \\ &\qquad \leq C(||b||^2_{L^2(\Omega)} + ||b||^3_{L^2(\Omega)} + ||\mathbf{f}||^2_{L^2(\Omega)}), \\ &||p||_{L^2(\Omega)} \leq C(||b||_{L^2(\Omega)} + ||b||^2_{L^2(\Omega)} + ||\mathbf{f}||_{L^2(\Omega)} \\ &\qquad\qquad + ||\mathbf{f}||^2_{L^2(\Omega)}). \end{aligned} \tag{14}$$

Here, C represents a positive constant.

3 Finite Element Discretization and Convergence

Henceforth, we make the assumption that Ω is a polygon in the case of $d = 2$ or polyhedron in the case of $d = 3$, allowing for complete meshing. For the space discretization, we consider a regular family of triangulations $(\mathcal{T}_h)_h$ of Ω, as decribed in [25], which is a set of closed non-degenerate triangles for $d = 2$ or tetrahedra for $d = 3$, called elements, satisfying,

- for each h, $\bar{\Omega}$ is the union of all elements of $\mathcal{T}_h$;
- the intersection of two distinct elements of $\mathcal{T}_h$ is either empty, a common vertex, or an entire common edge (or face when $d = 3$);
- the ratio of the diameter h_κ of an element $\kappa \in \mathcal{T}_h$ to the diameter ρ_κ of its inscribed circle when $d = 2$ or ball when $d = 3$ is bounded by a constant independent of h: there exists a positive constant σ independent of h such that,
$$\max_{\kappa\in\mathcal{T}_h} \frac{h_\kappa}{\rho_\kappa} \leq \sigma. \tag{15}$$

As is customary, h denotes the maximal diameter of all elements of $\mathcal{T}_h$. To define the finite element functions, let r denote a non-negative integer. For each κ in $\mathcal{T}_h$, we denote $\mathbb{P}_r(\kappa)$ the space of polynomials in d variables, restricted to κ, with a total degree at most 'r'. This notation extends to the faces or edges of κ. For every edge (when $d = 2$) or face (when $d = 3$) denoted as e in the mesh $\mathcal{T}_h$, we represent its diameter ash_e. In order to use inverse inequalities, we assume that the family of triangulations is uniformly regular in the following sense: there exists $\beta_0 > 0$ such that, for every element $\kappa \in \mathcal{T}_h$, we have

$$h_\kappa \geq \beta_0 h.$$

We will apply the following inverse inequality, [26]: for any dimension d, there exists a constant C_I such that, for any polynomial function v_h of degree r on κ on κ,

$$\|v_h\|_{L^3(\kappa)} \leq C_I h_\kappa^{-\frac{d}{6}} \|v_h\|_{L^2(\kappa)}. \tag{16}$$

The constant C_I depends on the regularity parameter σ from (15), but for the sake of simplicity, we omit this detail.

3.1 Discretization of the Variational Problem

In this section, we present the discretization of the variational problem, following the approach outlined in [10]. The authors of [10], introduced a discrete variational formulation for (13) using mixed elements, including the Raviart-Thomas mixed element, [27], and the Brezzi-Douglas-Marini mixed element, [28]. They also introduced an iterative scheme, although without a detailed investigation into its convergence, and provided numerical evidence demonstrating the convergence of the finite element approximation.

In this section, we consider the discrete variational formulation, introduce a new corresponding numerical algorithm and show the convergence of the corresponding iterative solution.
Let $X_h \subset X$ and $M_h \subset M$ the discrete spaces corresponding to the velocity and the pressure. We assume that they satisfy the following inf-sup condition:

$$\forall\, q_h \in M_h,\ \sup_{\mathbf{v}_h \in X_h} \frac{\displaystyle\int_\Omega q_h \operatorname{div}(\mathbf{v}_h)\, d\mathbf{x}}{\|\mathbf{v}_h\|_X} \geq \beta_p \|q_h\|_{M_h}, \tag{17}$$

where β_p is a positive constant independent of h.

Problem (13) can be discretized as follows:

$$\begin{cases} \forall \mathbf{v}_h \in X_h, \quad \dfrac{\mu}{\rho}\displaystyle\int_\Omega K^{-1}\mathbf{u}_h \cdot \mathbf{v}_h \, d\mathbf{x} \\ \quad +\dfrac{\beta}{\rho}\displaystyle\int_\Omega |\mathbf{u}_h|\mathbf{u}_h \cdot \mathbf{v}_h \, d\mathbf{x} - \int_\Omega p_h \operatorname{div}(\mathbf{v}_h)\, d\mathbf{x} \\ \quad = \displaystyle\int_\Omega \mathbf{f}\cdot \mathbf{v}_h \, d\mathbf{x}, \\ \forall q_h \in M_h, \quad \displaystyle\int_\Omega q_h \operatorname{div}(\mathbf{u}_h)\, d\mathbf{x} = \int_\Omega b q_h \, d\mathbf{x}. \end{cases} \tag{18}$$

In the following, we will consider for instance the Raviart-Thomas $RT0$ mixed element, [27], given by:

$$\begin{aligned} X_h =& \{\mathbf{v}_h \in X;\ \mathbf{v}_h(\mathbf{x})|_\kappa = a_\kappa \mathbf{x} + \mathbf{b}_\kappa, a_\kappa \in \mathbb{R}, \\ & \mathbf{b}_\kappa \in \mathbb{R}^d,\ \forall\, \kappa \in \mathcal{T}_h\}, \\ M_h =& \{q_h \in L^2(\Omega);\ \forall\, \kappa \in \mathcal{T}_h,\ q_h|_\kappa \text{ is constant}\}. \end{aligned} \tag{19}$$

It is also shown in [10], that there exists a unique $\mathbf{u}_{h,p} \in X_h$ such that

$$\forall q_h \in M_h, \quad \int_\Omega q_h \operatorname{div}(\mathbf{u}_{h,p})\, d\mathbf{x} = \int_\Omega b\, q_h d\mathbf{x}, \tag{20}$$

and $\mathbf{u}_{h,p}$ verifies the following bound,

$$||\mathbf{u}_{h,p}||_{X_p} \leq C_{l2}||b||_{L^2(\Omega)}. \tag{21}$$

It is shown in [10], that Problem (18) admits a unique solution $(\mathbf{u}_h, p_h) \in X_h \times M_h$ satisfying exactly similar bounds as (14). Also the solutions $(\mathbf{u}, p)$ of (13) and $(\mathbf{u}_h, p_h)$ of (18) verify the following *a priori* error:
If $(\mathbf{u}, p) \in W^{1,3}(\Omega)^d \times W^{1,3/2}(\Omega)$, then there exists a constant C independent of h such that

$$\begin{aligned} &||\mathbf{u} - \mathbf{u}_h||_{L^2(\Omega)} + ||\mathbf{u} - \mathbf{u}_h||^3_{3,\Omega} \leq Ch^2, \\ &||p - p_h||_{L^2(\Omega)} \leq Ch. \end{aligned} \tag{22}$$

An iterative algorithm: In order to approximate the solution of the non-linear problem (18), we introduce the following iterative algorithm: for a given initial guess $\mathbf{u}_h^0 \in X_h$ and having $\mathbf{u}_h^i$ at each iteration i, we compute $(\mathbf{u}_h^{i+1}, p_h^{i+1})$ solution of

$$\begin{cases} \forall \mathbf{v}_h \in X_h, \quad \alpha \displaystyle\int_\Omega (\mathbf{u}_h^{i+1} - \mathbf{u}_h^i)\mathbf{v}_h \\ \quad +\dfrac{\mu}{\rho}\displaystyle\int_\Omega K^{-1}\mathbf{u}_h^{i+1}\cdot \mathbf{v}_h \, d\mathbf{x} + \dfrac{\beta}{\rho}\int_\Omega |\mathbf{u}_h^i|\mathbf{u}_h^{i+1}\cdot \mathbf{v}_h \, d\mathbf{x} \\ \quad -\displaystyle\int_\Omega p_h^{i+1} \operatorname{div}(\mathbf{v}_h)\, d\mathbf{x} = \int_\Omega \mathbf{f}\cdot \mathbf{v}_h \, d\mathbf{x}, \\ \forall q_h \in M_h, \quad \displaystyle\int_\Omega q_h \operatorname{div}(\mathbf{u}_h^{i+1})\, d\mathbf{x} = \int_\Omega b q_h \, d\mathbf{x}, \end{cases} \tag{23}$$

where α is a given positive parameter.

In the following, we investigate the convergence of Scheme (23). We begin first by bounding the iterative solution when α is sufficiently big and the initial guess $\mathbf{u}_h^0$ is sufficiently close to $\mathbf{u}_{h,p}$.

Theorem 3.1. *Problem* (23) *admits a unique solution* $(\mathbf{u}_h^{i+1}, p_h^{i+1})$ *in* $X_h \times M_h$. *Furthermore, if the initial value* $\mathbf{u}_h^0$ *satisfies the condition*

$$||\mathbf{u}_h^0 - \mathbf{u}_{h,l}||_{L^2(\Omega)} \leq L_1(\mathbf{f}, \mathbf{u}_{h,p}), \tag{24}$$

where

$$\begin{aligned} L_1(\mathbf{f}, \mathbf{u}_{h,p}) = \Big(&\tfrac{2\rho}{\mu K_m}\big(\frac{3\rho}{2\mu K_m}||\mathbf{f}||^2_{L^2(\Omega)} \\ &+(\frac{\mu K_m}{6\rho} + \frac{3\mu K_M^2}{2\rho K_m})||\mathbf{u}_{h,p}||^2_{L^2(\Omega)} + \frac{4\beta}{3\rho}||\mathbf{u}_{h,p}||^3_{L^3(\Omega)}\big)\Big)^{1/2} \end{aligned} \tag{25}$$

and if α satisfies the condition

$$\alpha > 2\big(\frac{3\beta^2}{\rho\mu K_m}C_I^4 h^{-\frac{2d}{3}}||\mathbf{u}_{h,p}||^2_{L^3(\Omega)} + \frac{4\beta}{3\rho}C_I^3 h^{-d/2}L_2(\mathbf{f}, L_1(\mathbf{f},\mathbf{u}_{h,p}))^2\big), \tag{26}$$

where

$$L_2(\mathbf{f},\eta) = \frac{\rho}{\mu K_m}\big(\|\mathbf{f}\|_{L^2(\Omega)^d} + \frac{\mu K_M}{\rho}\|\mathbf{u}_{h,p}\|_{L^2(\Omega)} + \frac{\beta}{\rho}c_I^3 h^{-\frac{d}{2}}\|\mathbf{u}_{h,p}\|^2_{L^2(\Omega)} + \frac{\mu K_M}{\rho}\eta + \frac{\beta}{\rho}c_I^3 h^{-\frac{d}{2}}\eta^2\big).$$

then the solution of Problem (23) *satisfies the estimates*

$$||\mathbf{u}_h^{i+1} - \mathbf{u}_{h,p}||_{L^2(\Omega)} \le L_1(\mathbf{f},\mathbf{u}_{h,p}), \tag{27}$$

$$||\mathbf{u}_h^{i+1}||_{L^2(\Omega)} \le L_1(\mathbf{f},\mathbf{u}_{h,p}) + ||\mathbf{u}_{h,p}||_{L^2(\Omega)}, \tag{28}$$

and

$$||\mathbf{u}_h^{i+1}||^3_{L^3(\Omega)} \le (\frac{3\mu K_m}{2\beta} + \frac{3\alpha\rho}{2\beta})L_1^2(\mathbf{f},\mathbf{u}_{h,p}). \tag{29}$$

Proof. Problem (23) is a square linear system in finite dimension. Then to prove the existence and uniqueness of the corresponding solution, it suffices to prove the uniqueness. For a given $\mathbf{u}_h^i$, let $(\mathbf{u}_{h1}^{i+1}, p_{h1}^{i+1})$ and $(\mathbf{u}_{h2}^{i+1}, p_{h2}^{i+1})$ two different solutions of Problem (23) and $\mathbf{w}_h = \mathbf{u}_{h1}^{i+1} - \mathbf{u}_{h2}^{i+1}$ and $\xi_h = p_{h1}^{i+1} - p_{h2}^{i+1}$, then $(\mathbf{w}_h, \xi_h)$ is the solution of the following problem:

$$\begin{cases} \forall \mathbf{v}_h \in X_h, \quad \alpha\displaystyle\int_\Omega \mathbf{w}_h\mathbf{v}_h + \frac{\mu}{\rho}\int_\Omega K^{-1}\mathbf{w}_h\cdot\mathbf{v}_h\,d\mathbf{x} \\ \quad +\dfrac{\beta}{\rho}\displaystyle\int_\Omega |\mathbf{u}_h^i|\mathbf{w}_h\cdot\mathbf{v}_h\,d\mathbf{x} - \int_\Omega \xi_h\,\mathrm{div}(\mathbf{v}_h)\,d\mathbf{x} = 0, \\ \forall q_h \in M_h, \quad \displaystyle\int_\Omega q_h\,\mathrm{div}(\mathbf{w}_h)\,d\mathbf{x} = 0, \end{cases}$$

By taking $(\mathbf{v}_h, q_h) = (\mathbf{w}_h, \xi_h)$ and by remarking that $\dfrac{\beta}{\rho}\displaystyle\int_\Omega |\mathbf{u}_h^i||\mathbf{w}_h|^2\,d\mathbf{x} \ge 0$, we obtain by using the properties of K^{-1} the following bound:

$$(\alpha + \frac{K_m\mu}{\rho})||\mathbf{w}_h||^2_{L^2(\Omega)} \le 0.$$

Thus, we deduce that $\mathbf{w}_h = 0$. The inf-sup condition (17) deduces that $\xi_h = 0$ and then, we get the uniqueness of the solution of Problem (23).

Let us now prove the bound (27). We need first to bound the error $\|\mathbf{u}_h^{i+1} - \mathbf{u}_h^i\|_{L^2(\Omega)}$ with respect to the previous value $\mathbf{u}_h^i$. The second equation of Problem (23) allows us to deduce the relation

$$\forall q_h \in M_{u,h}, \quad \int_\Omega q_h\,\mathrm{div}(\mathbf{u}_h^{i+1} - \mathbf{u}_h^i)\,d\mathbf{x} = 0.$$

Then, the first equation of (23) with $\mathbf{v}_h = \mathbf{u}_h^{i+1} - \mathbf{u}_h^i$ gives

$$\begin{aligned} &\alpha\|\mathbf{u}_h^{i+1} - \mathbf{u}_h^i\|^2_{L^2(\Omega)} + \frac{\mu}{\rho}\int_\Omega K^{-1}\mathbf{u}_h^{i+1}\cdot(\mathbf{u}_h^{i+1} - \mathbf{u}_h^i)\,d\mathbf{x} \\ &+\frac{\beta}{\rho}\int_\Omega |\mathbf{u}_h^i|\mathbf{u}_h^{i+1}\cdot(\mathbf{u}_h^{i+1} - \mathbf{u}_h^i)\,d\mathbf{x} \\ &= \int_\Omega \mathbf{f}\cdot(\mathbf{u}_h^{i+1} - \mathbf{u}_h^i)\,d\mathbf{x}. \end{aligned}$$

By inserting $\mathbf{u}_h^i$ in the second and third terms of the last equation, we get,

$$\begin{aligned} &\alpha\left\|\mathbf{u}_h^{i+1} - \mathbf{u}_h^i\right\|^2_{L^2(\Omega)^d} + \tfrac{\mu}{\rho}\textstyle\int_\Omega K^{-1}|\mathbf{u}_h^{i+1} - \mathbf{u}_h^i|^2\,d\mathbf{x} \\ &+\frac{\beta}{\rho}\int_\Omega |\mathbf{u}_h^i||\mathbf{u}_h^{i+1} - \mathbf{u}_h^i|^2\,d\mathbf{x} \\ &= \int_\Omega \mathbf{f}\cdot(\mathbf{u}_h^{i+1} - \mathbf{u}_h^i)\,d\mathbf{x} - \frac{\mu}{\rho}\int_\Omega K^{-1}\mathbf{u}_h^i\cdot(\mathbf{u}_h^{i+1} - \mathbf{u}_h^i)\,d\mathbf{x} \\ &-\frac{\beta}{\rho}\int_\Omega |\mathbf{u}_h^i|\mathbf{u}_h^i\cdot(\mathbf{u}_h^{i+1} - \mathbf{u}_h^i)\,d\mathbf{x}. \end{aligned} \tag{30}$$

Using the properties of K^{-1}, the Cauchy-Schwartz inequality and relation (16) give the following

$$\begin{aligned} &\alpha\left\|\mathbf{u}_h^{i+1} - \mathbf{u}_h^i\right\|^2_{L^2(\Omega)^d} + \frac{\mu K_m}{\rho}\left\|\mathbf{u}_h^{i+1} - \mathbf{u}_h^i\right\|^2_{L^2(\Omega)^d} \\ &\le \|\mathbf{f}\|_{L^2(\Omega)^d}\left\|\mathbf{u}_h^{i+1} - \mathbf{u}_h^i\right\|_{L^2(\Omega)^d} \\ &\quad+\frac{\mu K_M}{\rho}\left\|\mathbf{u}_h^{i+1} - \mathbf{u}_h^i\right\|_{L^2(\Omega)^d}\left\|\mathbf{u}_h^i\right\|_{L^2(\Omega)^d} \\ &\quad+\frac{\beta}{\rho}C_I^3 h^{-d/2}\left\|\mathbf{u}_h^i\right\|^2_{L^2(\Omega)^d}\left\|\mathbf{u}_h^{i+1} - \mathbf{u}_h^i\right\|_{L^2(\Omega)^d}. \end{aligned} \tag{31}$$

We simplify by $\left\|\mathbf{u}_h^{i+1} - \mathbf{u}_h^i\right\|_{L^2(\Omega)^d}$ and insert $\mathbf{u}_{h,p}$ in the second member to obtain:

$$\|\mathbf{u}_h^{i+1} - \mathbf{u}_h^i\|_{L^2(\Omega)} \le L_2(\mathbf{f}, \|\mathbf{u}_h^i - \mathbf{u}_{h,p}\|^2_{L^2(\Omega)}), \tag{32}$$

where

$$L_2(\mathbf{f},\eta) = \frac{\rho}{\mu K_m}\big(\|\mathbf{f}\|_{L^2(\Omega)^d} + \frac{\mu K_M}{\rho}\|\mathbf{u}_{h,p}\|_{L^2(\Omega)} + \frac{\beta}{\rho}C_I^3 h^{-\frac{d}{2}}\|\mathbf{u}_{h,p}\|^2_{L^2(\Omega)} + \frac{\mu K_M}{\rho}\eta + \frac{\beta}{\rho}C_I^3 h^{-\frac{d}{2}}\eta^2\big).$$

Now, Relation (32) allows us to show (27). In fact, Property (20) allows us to deduce that the term $\mathbf{u}_{h,0}^{i+1} = \mathbf{u}_h^{i+1} - \mathbf{u}_{h,p}$ is in X_h and verifies

$$\forall q_h \in M_h, \quad \int_\Omega q_h\,\mathrm{div}(\mathbf{u}_{h,0}^{i+1})\,d\mathbf{x} = 0.$$

We consider the first equation of (23) with $\mathbf{v}_h = \mathbf{u}_{h,0}^{i+1} = \mathbf{u}_h^{i+1} - \mathbf{u}_{h,p}$ and we obtain:

$$\begin{aligned}
&\alpha \int_\Omega (\mathbf{u}_h^{i+1} - \mathbf{u}_h^i) \cdot (\mathbf{u}_h^{i+1} - \mathbf{u}_{h,p})\, d\mathbf{x} \\
&+\frac{\mu}{\rho}\int_\Omega K^{-1}|\mathbf{u}_h^{i+1} - \mathbf{u}_{h,p}|^2\, d\mathbf{x} + \frac{\beta}{\rho}\int_\Omega |\mathbf{u}_h^{i+1}|^3\, d\mathbf{x} \\
&= \int_\Omega \mathbf{f}\cdot(\mathbf{u}_h^{i+1} - \mathbf{u}_{h,p})\, d\mathbf{x} \\
&\qquad +\frac{\mu}{\rho}\int_\Omega K^{-1}\mathbf{u}_{h,p}\cdot(\mathbf{u}_h^{i+1} - \mathbf{u}_{h,p})\, d\mathbf{x} \\
&\qquad +\frac{\beta}{\rho}\int_\Omega (|\mathbf{u}_h^{i+1}| - |\mathbf{u}_h^i|)|\mathbf{u}_h^{i+1}|^2\, d\mathbf{x} \\
&\qquad +\frac{\beta}{\rho}\int_\Omega (|\mathbf{u}_h^i| - |\mathbf{u}_h^{i+1}|)\mathbf{u}_h^{i+1}\cdot\mathbf{u}_{h,p}\, d\mathbf{x} \\
&\qquad +\frac{\beta}{\rho}\int_\Omega |\mathbf{u}_h^{i+1}|\,\mathbf{u}_h^{i+1}\cdot\mathbf{u}_{h,p}\, d\mathbf{x}.
\end{aligned}$$

By inserting $\mathbf{u}_{h,p}$ in the first term of the last equation and using the properties of K we get:

$$\begin{aligned}
&\frac{\alpha}{2}||\mathbf{u}_h^{i+1} - \mathbf{u}_{h,p}||^2_{L^2(\Omega)} - \frac{\alpha}{2}||\mathbf{u}_h^i - \mathbf{u}_{h,p}||^2_{L^2(\Omega)} \\
&+\frac{\alpha}{2}||\mathbf{u}_h^{i+1} - \mathbf{u}_h^i||^2_{L^2(\Omega)} \\
&+\frac{\mu}{\rho}K_m||\mathbf{u}_h^{i+1} - \mathbf{u}_{h,p}||^2_{L^2(\Omega)} + \frac{\beta}{\rho}||\mathbf{u}_h^{i+1}||^3_{L^3(\Omega)} \\
&\quad \le ||\mathbf{f}||_{L^2(\Omega)}||\mathbf{u}_h^{i+1} - \mathbf{u}_{h,p}||_{L^2(\Omega)} \\
&\qquad +\frac{\mu}{\rho}K_M||\mathbf{u}_h^{i+1} - \mathbf{u}_{h,p}||_{L^2(\Omega)}||\mathbf{u}_{h,p}||_{L^2(\Omega)} \\
&\qquad +\frac{\beta}{\rho}||\mathbf{u}_h^i - \mathbf{u}_h^{i+1}||_{L^3(\Omega)}||\mathbf{u}_h^{i+1}||_{L^3(\Omega)}||\mathbf{u}_{h,p}||_{L^3(\Omega)} \\
&\qquad +\frac{\beta}{\rho}||\mathbf{u}_h^i - \mathbf{u}_h^{i+1}||_{L^3(\Omega)}||\mathbf{u}_h^{i+1}||^2_{L^3(\Omega)} \\
&\qquad +\frac{\beta}{\rho}||\mathbf{u}_h^{i+1}||^2_{L^3(\Omega)}||\mathbf{u}_{h,p}||_{L^3(\Omega)}.
\end{aligned}$$

We use the relation $a^2 b \le \frac{1}{3}\big(\frac{1}{\delta^3}b^3 + 2\delta^{3/2}a^3\big)$ (for any positive real numbers a and b) to obtain for any positive numbers $\varepsilon_i, i = 1,2,3$ and $\delta_j, j = 1,2$:

$$\begin{aligned}
&\frac{\alpha}{2}||\mathbf{u}_h^{i+1} - \mathbf{u}_{h,p}||^2_{L^2(\Omega)} - \frac{\alpha}{2}||\mathbf{u}_h^i - \mathbf{u}_{h,p}||^2_{L^2(\Omega)} \\
&+\frac{\alpha}{2}||\mathbf{u}_h^{i+1} - \mathbf{u}_h^i||^2_{L^2(\Omega)} \\
&+\frac{\mu}{\rho}K_m||\mathbf{u}_h^{i+1} - \mathbf{u}_{h,p}||^2_{L^2(\Omega)} + \frac{\beta}{\rho}||\mathbf{u}_h^{i+1}||^3_{L^3(\Omega)} \\
&\quad \le \frac{1}{2\varepsilon_1}||\mathbf{f}||^2_{L^2(\Omega)} + \frac{1}{2}\varepsilon_1||\mathbf{u}_h^{i+1} - \mathbf{u}_{h,p}||^2_{L^2(\Omega)} \\
&\quad +\frac{\mu^2}{2\rho^2\varepsilon_2}K_M^2||\mathbf{u}_{h,p}||^2_{L^2(\Omega)} + \frac{1}{2}\varepsilon_2||\mathbf{u}_h^{i+1} - \mathbf{u}_{h,p}||^2_{L^2(\Omega)} \\
&\quad +\frac{\beta^2}{2\rho^2\varepsilon_3}C_I^4 h^{-\frac{2d}{3}}||\mathbf{u}_{h,p}||^2_{L^3(\Omega)}||\mathbf{u}_h^i - \mathbf{u}_h^{i+1}||^2_{L^2(\Omega)} \\
&\quad +\frac{1}{2}\varepsilon_3(2||\mathbf{u}_h^{i+1} - \mathbf{u}_{h,p}||^2_{L^2(\Omega)} + 2||\mathbf{u}_{h,p}||^2_{L^2(\Omega)}) \\
&\quad +\frac{\beta}{3\rho}\big((\frac{1}{\delta_1})^3 C_I^3 h^{-d/2}||\mathbf{u}_h^{i+1} - \mathbf{u}_h^i||^3_{L^2(\Omega)} \\
&\qquad\qquad +2\delta_1^{3/2}||\mathbf{u}_h^{i+1}||^3_{L^3(\Omega)}\big) \\
&\quad +\frac{\beta}{3\rho}\big((\frac{1}{\delta_2})^3||\mathbf{u}_{h,p}||^3_{L^3(\Omega)} + 2\delta_2^{3/2}||\mathbf{u}_h^{i+1}||^3_{L^3(\Omega)}\big).
\end{aligned}$$

We choose $\varepsilon_1 = \varepsilon_2 = \dfrac{\mu K_m}{3\rho}$, $\varepsilon_3 = \dfrac{\mu K_m}{6\rho}$, $\delta_1 = \delta_2 = \big(\dfrac{1}{2}\big)^{2/3}$ and we denote:

$$\begin{aligned}
C_1(\|\mathbf{u}_h^i\|_{L^2(\Omega)}) &= \frac{\alpha}{2} - \frac{3\beta^2}{\rho\mu K_m}C_I^4 h^{-\frac{2d}{3}}||\mathbf{u}_{h,p}||^2_{L^3(\Omega)} \\
&\quad -\frac{4\beta}{3\rho}C_I^3 h^{-d/2}L_2(\mathbf{f}, \|\mathbf{u}_h^i - \mathbf{u}_{h,p}\|_{L^2(\Omega)}),
\end{aligned}$$

which is not necessarily positive at this level.
By using the bound (32), we get the following bound:

$$\begin{aligned}
&\frac{\alpha}{2}||\mathbf{u}_h^{i+1} - \mathbf{u}_{h,p}||^2_{L^2(\Omega)} - \frac{\alpha}{2}||\mathbf{u}_h^i - \mathbf{u}_{h,p}||^2_{L^2(\Omega)} \\
&+C_1(\|\mathbf{u}_h^i\|_{L^2(\Omega)})||\mathbf{u}_h^{i+1} - \mathbf{u}_h^i||^2_{L^2(\Omega)} \\
&+\frac{\mu K_m}{2\rho}||\mathbf{u}_h^{i+1} - \mathbf{u}_{h,p}||^2_{L^2(\Omega)} + \frac{\beta}{3\rho}||\mathbf{u}_h^{i+1}||^3_{L^3(\Omega)} \\
&\quad \le \frac{3\rho}{2\mu K_m}||\mathbf{f}||^2_{L^2(\Omega)} + \frac{4\beta}{3\rho}||\mathbf{u}_{h,p}||^3_{L^3(\Omega)} \\
&\qquad +(\frac{\mu K_m}{6\rho} + \frac{3\mu K_M^2}{2\rho K_m})||\mathbf{u}_{h,p}||^2_{L^2(\Omega)} \\
&\quad \le \frac{\mu K_m}{2\rho}L_1^2(\mathbf{f}, \mathbf{u}_{h,p}).
\end{aligned} \tag{33}$$

We now prove estimate (27) by induction on i under some conditions on α. Starting with relation (24), we suppose that we have

$$||\mathbf{u}_h^i - \mathbf{u}_{h,p}||_{L^2(\Omega)} \le L_1(\mathbf{f}, \mathbf{u}_{h,p}). \quad (34)$$

We are in one of the following two situations:

- We have $||\mathbf{u}_h^{i+1} - \mathbf{u}_{h,l}||_{L^2(\Omega)} \le ||\mathbf{u}_h^i - \mathbf{u}_{h,l}||_{L^2(\Omega)}$. We obviously deduce the bound

$$||\mathbf{u}_h^{i+1} - \mathbf{u}_{h,l}||_{L^2(\Omega)} \le L_1(\mathbf{f}, \mathbf{u}_{h,l}),$$

  from the induction hypothesis

- We have $||\mathbf{u}_h^{i+1} - \mathbf{u}_{h,l}||_{L^2(\Omega)} \ge ||\mathbf{u}_h^i - \mathbf{u}_{h,l}||_{L^2(\Omega)}$. By using the induction condition (34) and the fact that the function L_2 is increasing with respect to η, we chose

$$\begin{aligned}\frac{\alpha}{2} \ge & \frac{3\beta^2}{\rho\mu K_m} C_I^4 h^{-\frac{2d}{3}} ||\mathbf{u}_{h,l}||^2_{L^3(\Omega)} \\ & + \frac{4\beta}{3\rho} C_I^3 h^{-d/2} L_2(\mathbf{f}, L_1(\mathbf{f}, \mathbf{u}_{h,l})),\end{aligned} \quad (35)$$

  and we get

$$\begin{aligned}\frac{\alpha}{2} \ge & \frac{3\beta^2}{\rho\mu K_m} C_I^4 h^{-\frac{2d}{3}} ||\mathbf{u}_{h,l}||^2_{L^3(\Omega)} \\ & + \frac{4\beta}{3\rho} C_I^3 h^{-d/2} L_2(\mathbf{f}, ||\mathbf{u}_h^i - \mathbf{u}_{h,l}||_{L^2(\Omega)}),\end{aligned} \quad (36)$$

  which leads to $C_1(||\mathbf{u}_h^i||_{L^2(\Omega)}) \ge 0$, and then

$$||\mathbf{u}_h^{i+1} - \mathbf{u}_{h,l}||_{L^2(\Omega)} \le L_1(\mathbf{f}, \mathbf{u}_{h,l}).$$

whence we deduce relation (27).
The bound (28) is a simple consequence of (27) by using a simple triangle inequality. The inequality (29) can be easily obtained by using Equation (33) and Relation (27). □

Remark 3.2. *It's worth noting that the bounds of the iterative velocity* (23) *are derived under the condition* (26)*, where α must satisfy a certain constraint that is not straightforward to compute. This constraint depends on $h^{-2d/3}$. In the final section, we will provide numerical simulations and explore how the convergence depends on α in specific cases.*

Remark 3.3. *Relation* (24) *assumes that the initial guess $\mathbf{u}_h^0$ must lie within a ball centered at $\mathbf{u}_{h,p}$ with a radius of $L_1(\mathbf{f}, \mathbf{u}_{h,p})$, which is not known. However, upon inspecting the expression for $L_1(\mathbf{f}, \mathbf{u}_{h,p})$ provided in* (25)*, we can deduce that the initial guess $\mathbf{u}_h^0 = \mathbf{0}$ satisfies Relation* (24)*.*

The next theorem treats the convergence of the solution of Scheme (23).

Theorem 3.4. *Under the assumptions of Theorem* 3.1 *and if α satisfies also the condition*

$$\alpha > \frac{\rho C^2}{K_m \mu} h^{-d}, \quad (37)$$

where

$$C = \frac{\beta}{\rho} C_I^3 \big(L_1(\mathbf{f}, \mathbf{u}_{h,l}) + \|\mathbf{u}_{h,l}\|_{L^2(\Omega)} \big)$$

then the iterative solutions $(\mathbf{u}_h^i, p_h^i)$ of Problem (23) *converges in $L^2(\Omega)^d \times L^2(\Omega)$ to the solution $(\mathbf{u}_h, p_h)$ of Problem* (18)*.*

Proof. We take the difference between the equations (18) and (23) with $\mathbf{v}_h = \mathbf{u}_h^{i+1} - \mathbf{u}_h$, resulting in

$$\begin{aligned}&\frac{\alpha}{2}||\mathbf{u}_h^{i+1} - \mathbf{u}_h||^2_{L^2(\Omega)} - \frac{\alpha}{2}||\mathbf{u}_h^i - \mathbf{u}_h||^2_{L^2(\Omega)} \\ &+ \frac{\alpha}{2}||\mathbf{u}_h^{i+1} - \mathbf{u}_h^i||^2_{L^2(\Omega)} + \frac{\mu}{\rho}\int_\Omega K^{-1}(\mathbf{u}_h^{i+1} - \mathbf{u}_h)^2\, d\mathbf{x} \\ &+ \frac{\beta}{\rho}(|\mathbf{u}_h^i|\mathbf{u}_h^{i+1} - |\mathbf{u}_h|\mathbf{u}_h, \mathbf{u}_h^{i+1} - \mathbf{u}_h) = 0.\end{aligned}$$

The last term in the previous equation, denoted by T, can be decomposed into

$$\begin{aligned}T = & \frac{\beta}{\rho}((|\mathbf{u}_h^i| - |\mathbf{u}_h^{i+1}|)\mathbf{u}_h^{i+1}, \mathbf{u}_h^{i+1} - \mathbf{u}_h) \\ & + \frac{\beta}{\rho}(|\mathbf{u}_h^{i+1}|\mathbf{u}_h^{i+1} - |\mathbf{u}_h|\mathbf{u}_h, \mathbf{u}_h^{i+1} - \mathbf{u}_h).\end{aligned}$$

We denote by T_1 and T_2, respectively the first and the second terms in the right-hand side of the last equation. Using (12), we have $T_2 \ge 0$. Then, by using (16) and (4), we have

$$\begin{aligned}&\frac{\alpha}{2}||\mathbf{u}_h^{i+1} - \mathbf{u}_h||^2_{L^2(\Omega)} - \frac{\alpha}{2}||\mathbf{u}_h^i - \mathbf{u}_h||^2_{L^2(\Omega)} \\ &+ \frac{\alpha}{2}||\mathbf{u}_h^{i+1} - \mathbf{u}_h^i||^2_{L^2(\Omega)} + \frac{K_m\mu}{\rho}\|\mathbf{u}_h^{i+1} - \mathbf{u}_h\|^2_{L^2(\Omega)} + T_2 \\ &\le |T_1| \\ &\le \frac{\beta}{\rho}\int_\Omega |\mathbf{u}_h^{i+1} - \mathbf{u}_h^i|\,|\mathbf{u}_h^{i+1}|\,|\mathbf{u}_h^{i+1} - \mathbf{u}_h| d\mathbf{x} \\ &\le \frac{\beta}{\rho}||\mathbf{u}_h^{i+1} - \mathbf{u}_h^i||_{L^3(\Omega)}\, ||\mathbf{u}_h^{i+1}||_{L^3(\Omega)}\, ||\mathbf{u}_h^{i+1} - \mathbf{u}_h||_{L^3(\Omega)} \\ &\le \frac{\beta}{\rho} C_I^3 h^{-\frac{d}{2}} ||\mathbf{u}_h^{i+1} - \mathbf{u}_h^i||_{L^2(\Omega)}\, ||\mathbf{u}_h^{i+1}||_{L^2(\Omega)} \\ &\qquad ||\mathbf{u}_h^{i+1} - \mathbf{u}_h||_{L^2(\Omega)} \\ &\le \frac{\beta}{\rho} C_I^3 h^{-\frac{d}{2}} \big(L_1(\mathbf{f}, \mathbf{u}_{h,l}) + \|\mathbf{u}_{h,p}\|_{L^2(\Omega)} \big) \\ &\qquad ||\mathbf{u}_h^{i+1} - \mathbf{u}_h^i||_{L^2(\Omega)}\, ||\mathbf{u}_h^{i+1} - \mathbf{u}_h||_{L^2(\Omega)}.\end{aligned}$$

Here, we denote $C = \dfrac{\beta}{\rho} C_I^3 \big(L_1(\mathbf{f}, \mathbf{u}_{h,l}) + ||\mathbf{u}_{h,l}||_{L^2(\Omega)} \big)$ and use the inequality $ab \le \dfrac{1}{2\varepsilon}a^2 + \dfrac{\varepsilon}{2}b^2$ (with $\varepsilon = \dfrac{K_m \mu}{\rho}$) to obtain the following bound :

$$\begin{aligned}
&\frac{\alpha}{2}||\mathbf{u}_h^{i+1} - \mathbf{u}_h||^2_{L^2(\Omega)} - \frac{\alpha}{2}||\mathbf{u}_h^{i} - \mathbf{u}_h||^2_{L^2(\Omega)} \\
&+\frac{\alpha}{2}||\mathbf{u}_h^{i+1} - \mathbf{u}_h^i||^2_{L^2(\Omega)} + \frac{K_m\mu}{2\rho}||\mathbf{u}_h^{i+1} - \mathbf{u}_h||^2_{L^2(\Omega)} \\
&\qquad \le \frac{\rho C^2}{2K_m\mu} h^{-d} ||\mathbf{u}_h^{i+1} - \mathbf{u}_h^i||^2_{L^2(\Omega)}.
\end{aligned}$$

We choose

$$\alpha > \frac{\rho C^2}{K_m \mu} h^{-d}, \tag{38}$$

denote by $C_1(h) = \dfrac{1}{2}(\alpha - \dfrac{\rho C^2}{K_m\mu} h^{-d})$ and obtain

$$\begin{aligned}
&\frac{\alpha}{2}||\mathbf{u}_h^{i+1} - \mathbf{u}_h||^2_{L^2(\Omega)} - \frac{\alpha}{2}||\mathbf{u}_h^{i} - \mathbf{u}_h||^2_{L^2(\Omega)} \\
&+C_1(h)||\mathbf{u}_h^{i+1} - \mathbf{u}_h^i||^2_{L^2(\Omega)} + \frac{\mu K_m}{2\rho}||\mathbf{u}_h^{i+1} - \mathbf{u}_h||^2_{L^2(\Omega)} \\
&\le 0.
\end{aligned} \tag{39}$$

We deduce then that if $||\mathbf{u}_h^i - \mathbf{u}_h||_{L^2(\Omega)} \neq 0$ and for all integer i we have:

$$||\mathbf{u}_h^{i+1} - \mathbf{u}_h||_{L^2(\Omega)} < ||\mathbf{u}_h^{i} - \mathbf{u}_h||_{L^2(\Omega)},$$

and we deduce the convergence of the sequence $(\mathbf{u}_h^{i+1} - \mathbf{u}_h)$ in $L^2(\Omega)^d$ and then the convergence of $\mathbf{u}_h^i$ to $\mathbf{u}_h$ in $L^2(\Omega)^d$.
Now, we prove the convergence of the iterative pressure. We take the difference between the equations (18) and (23) and we obtain for all $\mathbf{v}_h \in X_h$ the equation

$$\begin{aligned}
&\int_\Omega (p_h^{i+1} - p_h)\, \mathrm{div}(\mathbf{v}_h)\, d\mathbf{x} \\
&= \alpha \int_\Omega (\mathbf{u}_h^{i+1} - \mathbf{u}_h^i)\mathbf{v}_h\, d\mathbf{x} - \frac{\mu}{\rho}\int_\Omega K^{-1}(\mathbf{u}_h - \mathbf{u}_h^{i+1})\mathbf{v}_h\, d\mathbf{x} \\
&\quad -\frac{\beta}{\rho}((|\mathbf{u}_h| - |\mathbf{u}_h^i|)\mathbf{u}_h, \mathbf{v}_h) - \frac{\beta}{\rho}(|\mathbf{u}_h^i|(\mathbf{u}_h - \mathbf{u}_h^{i+1}), \mathbf{v}_h).
\end{aligned}$$

By applying the inverse inequality (16), we obtain the following:

$$\begin{aligned}
&\frac{\left| \int_\Omega (p_h^{i+1} - p_h)\, \mathrm{div}(\mathbf{v}_h)\, d\mathbf{x} \right|}{||\mathbf{v}_h||_X} \\
&\le \Big(\alpha ||\mathbf{u}_h^i - \mathbf{u}_h^{i+1}||_{L^2(\Omega)} \\
&\qquad + \frac{\mu K_m}{\rho}||\mathbf{u}_h - \mathbf{u}_h^{i+1}||_{L^2(\Omega)} \Big) \frac{||\mathbf{v}_h||_{L^2(\Omega)}}{||\mathbf{v}_h||_X} \\
&\qquad + \frac{\beta}{\rho} C_I h^{-\frac{d}{6}} ||\mathbf{u}_h - \mathbf{u}_h^i||_{L^2(\Omega)} \\
&\qquad\qquad (||\mathbf{u}_h||_{L^3(\Omega)} + ||\mathbf{u}_h^i||_{L^3(\Omega)}) \frac{||\mathbf{v}_h||_{L^3(\Omega)}}{||\mathbf{v}_h||_X}.
\end{aligned}$$

Since we have $||\mathbf{v}_h||_{L^3(\Omega)} \le ||\mathbf{v}_h||_X$ and $||\mathbf{v}_h||_{L^2(\Omega)} \le |\Omega|^{1/6}||\mathbf{v}_h||_{L^3(\Omega)}$, we deduce, by using the inf-sup condition (17), the following relation

$$\begin{aligned}
&||p_h^{i+1} - p_h||_{L^2(\Omega)} \\
&\le \frac{1}{\beta_p}\Big(\alpha |\Omega|^{1/6} ||\mathbf{u}_h^i - \mathbf{u}_h^{i+1}||_{L^2(\Omega)} \\
&\qquad + |\Omega|^{1/6} \frac{\mu K_m}{\rho} ||\mathbf{u}_h - \mathbf{u}_h^{i+1}||_{L^2(\Omega)} \\
&\qquad + \frac{\beta}{\rho} C_I h^{-\frac{d}{6}} ||\mathbf{u}_h - \mathbf{u}_h^i||_{L^2(\Omega)^d} \\
&\qquad\qquad (||\mathbf{u}_h||_{L^3(\Omega)^d} + ||\mathbf{u}_h^i||_{L^3(\Omega)^d}) \Big).
\end{aligned}$$

Thus, the strong convergence of $\mathbf{u}_h^i$ to $\mathbf{u}_h$ in $L^2(\Omega)^d$ implies the strong convergence of p_h^i to p_h in $L^2(\Omega)$.□

Remark 3.5. *In order to show the convergence of the algorithm* (23)*, the assumptions of Theorems 3.1 and 3.4 require the conditions* (26) *and* (37)*. These conditions demand that γ must exceed a certain constant that is difficult to compute and relies on the mesh step h.*

4 Numerical Results

In this section, we present numerical experiments corresponding to Scheme (23). These simulations were performed using the FreeFem++ code developed [29].
Two cases are considered in this work: First, we assess the convergence properties of the method by using the standard mesh refinement analysis.
The second example involves a more complicated geometry (Figure 3) presenting reentrant corners.

4.1 First Test Case: Convergence Analysis

We consider the domain $\Omega = (0,1)^2 \subset \mathbf{R}^2$ where each edge is divided into N equal segments. Then

Ω is divided into N^2 equal squares and equivalently into $2N^2$ equal triangles. For simplicity, we set $\mu = \rho = 1$ and $K = I$.

To determine the convergence of the iterative problem (23), we employ the stopping criterion $Err_L \leq \varepsilon$ where ε is a given tolerance considered in this work equal to 10^{-5} and Err_L is defined as follows:

$$Err_L = \sqrt{\frac{||\mathbf{u}_h^{i+1} - \mathbf{u}_h^i||^2_{L^2(\Omega)} + ||p_h^{i+1} - p_h^i||^2_{L^2(\Omega)}}{||\mathbf{u}_h^{i+1}||^2_{L^2(\Omega)} + ||p_h^{i+1}||^2_{L^2(\Omega)}}}.$$

Regarding the initial guess $\mathbf{u}_h^0$, we consider two situations:

1. $\mathbf{u}_h^0 = \mathbf{0}$.
2. $\mathbf{u}_h^0 = \mathbf{u}_{h,d}^0$ is calculated by using Darcy's problem which corresponds to $\beta = \alpha = 0$.

We will later observe that the second case, where $\mathbf{u}_h^0 = \mathbf{u}_{h,d}^0$, leads to improved convergence of the algorithms.
Additionally, we compute the error

$$Err = \sqrt{\frac{||\mathbf{u}_h^i - \mathbf{u}||^2_{L^2(\Omega)} + ||p_h^i - p||^2_{L^2(\Omega)}}{||\mathbf{u}||^2_{L^2(\Omega)} + ||p||^2_{L^2(\Omega)}}}$$

where $(\mathbf{u}, p)$ is the exact solution of problem (13). This error provides information about the convergence of the algorithm (23).

In fact, to compute the solution of the iterative problem (23), we use the penalty method ([29]) which consists to solve the following problem:

$$\begin{cases} \forall \mathbf{v}_h \in X_h, \quad \displaystyle\int_\Omega \alpha(\mathbf{u}_h^{i+1} - \mathbf{u}_h^i) \cdot \mathbf{v}_h \, d\mathbf{x} \\ +\displaystyle\frac{\mu}{\rho}\int_\Omega K^{-1}\mathbf{u}_h^{i+1} \cdot \mathbf{v}_h \, d\mathbf{x} + \frac{\beta}{\rho}\int_\Omega |\mathbf{u}_h^i|\mathbf{u}_h^{i+1} \cdot \mathbf{v}_h \, d\mathbf{x} \\ -\displaystyle\int_\Omega p_h^{i+1} \operatorname{div}(\mathbf{v}_h) \, d\mathbf{x} = \int_\Omega \mathbf{f} \cdot \mathbf{v}_h \, d\mathbf{x}, \\ \forall q_h \in M_h, \quad \displaystyle\int_\Omega q_h \operatorname{div}(\mathbf{u}_h^{i+1}) \, d\mathbf{x} + \varepsilon_p \int_\Omega p_h^{i+1} q_h \, d\mathbf{x} \\ \qquad = \displaystyle\int_\Omega b q_h \, d\mathbf{x}, \end{cases} \tag{40}$$

where $\varepsilon_p = 10^{-8}$.
The numerical algorithm solving Problem (40) can be summarized in a standard way as follows: set $\mathbf{u}_h^0 = 0$,

(1) having $\mathbf{u}_h^i$,
  (a) Solve the problem (40) to compute $(\mathbf{u}_h^{i+1}, p_h^{i+1})$.
  (b) Calculate E_{rrL}.

(2)
- If $E_{rrL} \leq \varepsilon$, we stop the algorithm.
- else set $\mathbf{u}_h^i = \mathbf{u}_h^{i+1}$ and $i = i + 1$ and then go to (1).

We propose the following two examples :

1. First example:

$$\begin{cases} p(x,y) = 10\sin(\pi x)\sin(\pi y), \\ \mathbf{u}(x,y) = \gamma(\exp(x)\,\sin(\pi y), \dfrac{1}{\pi}\exp(x)\,\cos(\pi y))^T, \\ b = 0, \\ \mathbf{f} = \mathbf{u} + \beta|\mathbf{u}|\mathbf{u} + \nabla p, \end{cases} \tag{41}$$

2. Second example:

$$\begin{cases} p(x,y) = 10(x - x^2)(y - y^2), \\ \mathbf{u}(x,y) = \gamma(x\exp(\pi y), y\exp(\pi x))^T, \\ b = \gamma(\exp(\pi x) + \exp(\pi y)), \\ \mathbf{f} = \mathbf{u} + \beta|\mathbf{u}|\mathbf{u} + \nabla p, \end{cases} \tag{42}$$

Where γ is a real parameter.

To study the dependency of the convergence on the parameter α, we consider $N = 60, \beta = 20$ and $\gamma = 20$. For each α, we stop the algorithm (23) when $Err_L < 1e^{-5}$. We consider that the algorithms doesn't converge if this condition is not reached after 10000 iterations.

Table 1 and Table 2 display the error Err and the number of iterations Nbr which describe the convergence of Algorithm (23) with respect to α for each example when $\mathbf{u}_h^0 = \mathbf{0}$. It is observed that Algorithm (23) converges for Example (41) for all considered values of α, with the best convergence archived for $\alpha = 1000$. In the case of Example (42), it converges for $\alpha > 10$, with the best convergence again observed for $\alpha = 1000$.

Table 3 and Table 4 show, for $\mathbf{u}_h^0 = \mathbf{u}_{h,d}^0$ computed with the Darcy's problem, the error Err and the number of iterations Nbr which describe the convergence of Algorithm (23) with respect to α, for each example. In this case, we remark also that Algorithm (23) consistently converges always, and the best convergence is for $\alpha = 100$ for Example (41) and $\alpha = 1000$ for Example (42). One significant

Table 1. Error Err (in logarithmic scale) and number of iterations Nbr for $\mathbf{u}_h^0 = \mathbf{0}$, with respect to α associated to Example (41) of Algorithm (23). ($\beta = 20$ and $\gamma = 20$).

α	**.1**	**1**	**10**	**100**	**1000**
Nbr	7376	3020	487	61	45
Err	-1.43	-1.43	-1.43	-1.43	-1.43

Table 2. Error Err (in logarithmic scale) and number of iterations Nbr for $\mathbf{u}_h^0 = \mathbf{0}$ and for each α associated to Example (42) of Algorithm (23). ($\beta = 20$ and $\gamma = 20$).

α	**.1**	**1**	**10**	**100**	**1000**
Nbr	>10000	>10000	3518	512	69
Err	div	div	-0.36	-0.36	-0.36

advantage when using $\mathbf{u}_h^0 = \mathbf{u}_{h,d}^0$ computed with the Darcy's problem is that Nbr is lower compared to when $\mathbf{u}_h^0 = \mathbf{0}$.

Table 3. Error Err (in logarithmic scale) and number of iterations Nbr for $\mathbf{u}_h^0 = \mathbf{u}_{h,d}^0$ and for each α associated to Example (41) of Algorithm (23). ($\beta = 20$ and $\gamma = 20$).

α	**.01**	**.1**	**1**	**10**	**100**	**1000**
Nbr	1214	1038	463	104	18	20
Err	-1.43	-1.43	-1.43	-1.43	-1.43	-1.43

Table 4. Error Err (in logarithmic scale) and number of iterations Nbr for $\mathbf{u}_h^0 = \mathbf{u}_{h,d}^0$ and for each α associated to Example (42) of Algorithm (23). ($\beta = 20$ and $\gamma = 20$).

α	**.01**	**.1**	**1**	**10**	**100**	**1000**
Nbr	7526	6781	3632	868	149	25
Err	-0.36	-0.36	-0.36	-0.36	-0.36	-0.36

For further study, we take $N = 60$, $\beta = 10$, $\gamma = 1$, and we consider the initial guess $\mathbf{u}_h^0 = \mathbf{u}_{hd}^0$. Table 5 and Table 6 show the error Err and the number of iterations Nbr for each α and each example. We notice that the best convergence (in term of number of iterations) is obtained for $\alpha = 1000$ for Example (41) and for $\alpha = 100$ for Example (42).

Table 5. Error Err (in logarithmic scale) and number of iterations Nbr for each α associated to Example (41) of Algorithm (23). ($\beta = 10$ and $\gamma = 1$).

α	**.01**	**.1**	**1**	**10**	**100**	**1000**
Nbr	26	22	9	4	4	2
Err	-1.72	-1.72	-1.72	-1.72	-1.72	-1.72

Table 6. Error Err (in logarithmic scale) and number of iterations Nbr for each α associated to Example (42) of Algorithm (23). ($\beta = 10$ and $\gamma = 1$).

α	**.01**	**.1**	**1**	**10**	**100**	**1000**
Nbr	481	376	181	40	17	59
Err	-0.96	-0.96	-0.96	-0.96	-0.96	-0.96

Figure 1 and Figure 2 show, for $\alpha = 10$ and $\gamma = 1$ and $\beta = 10$, in logarithmic scale the error Err with respect to $h = \frac{1}{N}$, $N = 60, \ldots, 200$, for the algorithm (23) (first example in Figure 1 and second example in 2). The slopes of the error lines are 0.983 for the first example and 1.10 for the second one, which are close to the theoretical slope equal to 1.

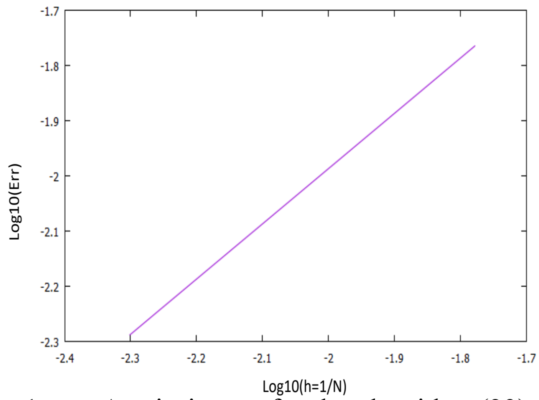

Fig. 1: A priori error for the algorithm (23) with respect to $h = 1/N$: first example. ($\beta = 10$ and $\gamma = 1$)

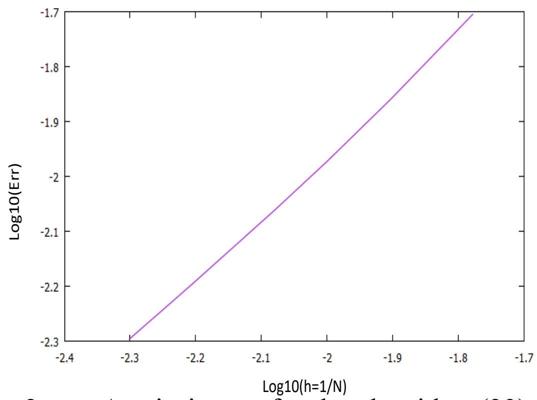

Fig. 2: A priori error for the algorithm (23) with respect to $h = 1/N$: second example. ($\beta = 10$ and $\gamma = 1$)

Remark 4.1. *We can list the following comments:*

DOI: 10.37394/232012.2024.19.11

1. *Table 1, Table 2, Table 3, Table 4, Table 5 and Table 6 show that for the examples considered,a large value of α corresponds to a relatively small number of iterations in the algorithm. However, determining the optimal value of α for minimal iterations in advance is challenging. Additionally, using the initial guess $\mathbf{u}_h^0 = \mathbf{u}_{h,d}^0$ computed with the Darcy problem consistently produces better results than using $\mathbf{u}_h^0 = \mathbf{0}$.*

2. *The slopes of the curves presented in Figure 1 are close to the theoretical one (equal to 1).*

4.2 Second Test Case

In this part, we consider numerical results for a more complicated geometry (Figure 3) with Problem (13) by the numerical scheme (23). The domain features reentrant corners to highlight the fluctuations around these parts of the geometry. In all the numerical results considered in this section, we set $\mu = \rho = 1$, $\alpha = 10$, $\mathbf{f} = (f, 0)$ where

$$f = \begin{cases} 0 & \text{if } y > 1, \\ -2 & \text{if } y <= 1, \end{cases}$$

and

$$K^{-1} = \begin{pmatrix} k_{11} & k_{12} \\ k_{21} & k_{22} \end{pmatrix}$$

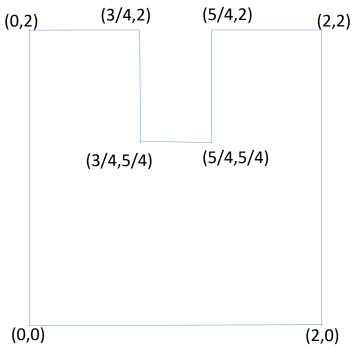

Fig. 3: Geometry

To illustrate the difference between Darcy ($\alpha = \beta = 0$) and Darcy-Forchheimer ($\alpha = 10, \beta = 10$), Figure 5 and Figure 6 show comparisons of the velocity and pressure. We observe the difference between these two cases, where, in the Darcy case, the fluid is more agitated than in the Darcy-Forchheimer case.

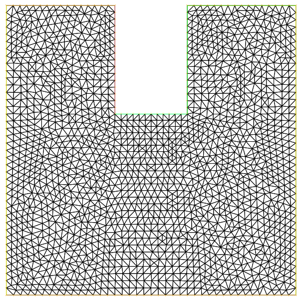
Fig. 4: Mesh

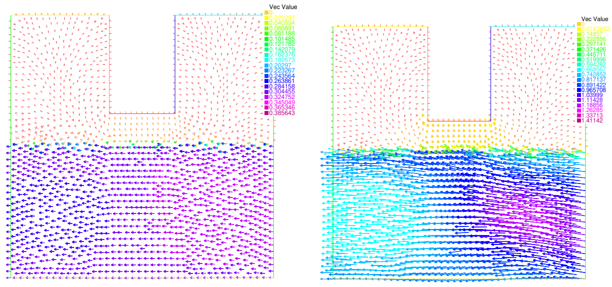
Fig. 5: Velocity: Darcy-Forchheimer on the left ($\beta = \alpha = 10$) and Darcy on the right ($\beta = \alpha = 0$)

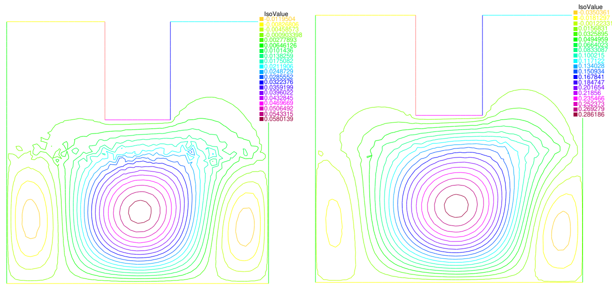
Fig. 6: Pressure: Darcy-Forchheimer on the left ($\beta = \alpha = 10$) and Darcy on the right ($\beta = \alpha = 0$)

5 Conclusion and Perspective

In this study, we have addressed the Darcy-Forchheimer problem with pressure boundary condition. We first introduced the weak formulation and showed the upper bound of the corresponding solution. Then, by utilizing the Raviart-Thomas $RT0$ mixed finite elements, we have discretized the system and then introduced an iterative scheme to solve the resulting nonlinear discrete problem. Our study has effectively demonstrated the well-posedness and convergence of this iterative approach. Furthermore, our numerical experiments have provided evidence supporting the effectiveness and accuracy of the proposed numerical scheme.
This work can be extended in several directions, such as coupling the Darcy-Forchheimer system with a pressure boundary condition to the heat equation or coupling it with the Stokes or Navier-Stokes equations, among others.

References:

[1] Neuman S.P., Theoretical derivation of Darcy's law, *Acta Mech. 25(3), 153-170 (1977).*

[2] Whitaker S., Flow in porous media I: A theoretical derivation of Darcy's law, *Transp. Porous Media 1(1), 3-25 (1986).*

[3] Forchheimer P., Wasserbewegung durch Boden, *Z. Ver. Deutsh. Ing. 45, 1782-1788 (1901).*

[4] Ruth D., Ma H., On the derivation of the Forchheimer equation by means of the averaging theorem, *Transp. Porous Media 7(3), 255-264 (1992).*

[5] Girault V., Wheeler M.F., Numerical discretization of a Darcy-Forchheimer model, *Numer. Math. 110(2), 161-198 (2008).*

[6] Lopez H., Molina B., Jose J.S., Comparison between different numerical discretizations for a Darcy-Forchheimer model, *Electron. Trans. Numer. Anal. 34, 187-203 (2009).*

[7] Salas J.J., Lopez H., Molina B., An analysis of a mixed finite element method for a Darcy-Forchheimer model, *Mathematical and Computer Modelling 57, 2325-2338 (2013).*

[8] Sayah T., Semaan, Triki F., A Posteriori Error estimates for Darcy-Forchheimer's Problem, *Computational Methods in Applied Mathematics, 23 (2), 517-544, (2023).*

[9] Sayah T., Semaan G., Triki F., Finite element methods for the Darcy-Forchheimer problem coupled with the convection-diffusion-reaction problem, *ESAIM Math. Model. Numer. Anal. 55(6), 2643-2678, (2021).*

[10] Pan H., Rui H., Mixed Element Method for Two-Dimensional Darcy-Forchheimer Model, *J. Sci. Comput. 52, 563-587, (2012).*

[11] Aghaei-Jouybari, M., Seo, J.-H., Pinto, S., Cattafesta, L., Meneveau, C., Mittal, R., Extended Darcy–Forchheimer law including inertial flow deflection effects. Journal of Fluid Mechanics, 980, A13. doi:10.1017/jfm.2023.1083 (2024)

[12] Akyildiz F.T., Alshammari F.S. and Tunç C., Novel Numerical Investigations of Some Problems Based on the Darcy–Forchheimer Model and Heat Transfer, *Mathematics, 12(11), (2024).*

[13] ALEJANDRO ALLENDES A., CAMPA G. AND OTAROLA E., Numerical Discretization of a Darcy-Forchheimer Problem Coupled with a Singular Heat Equation, *SIAM Journal on Scientific Computing, 45(5), (2023).*

[14] Dehghan M., Gharibi Z., A fully mixed virtual element method for Darcy–Forchheimer miscible displacement of incompressible fluids appearing in porous media, IMA Journal of Numerical Analysis, Volume 44, Issue 2, March 2024, Pages 797–835

[15] Granero-Belinchón R.and Scrobogna S., Asymptotic models for free boundary flow in porous media. Physica D: Nonlinear Phenomena. 392, 1-16, (2019).

[16] Huang J., Yue Z., Zhang J., Fu K., Feng X., Numerical discretization of a Darcy–Forchheimer flow with variable density and heat transfer, *Journal of Computational and Applied Mathematics, 457, (2025).*

[17] Li A., Huang J,, Liu W., Wei H., Yi N., A characteristic block-centered finite difference method for Darcy–Forchheimer compressible miscible displacement problem, *Journal of Computational and Applied Mathematics, 413, (2022).*

[18] Grosan T., Pop I., Patrulescu, F. O., Transfer Phenomena in Non-Darcy Bidisperse Porous Media, *WSEAS Transactions on Heat and Mass Transfer, 14, 147-152, (2019).*

[19] Li S., Khan M., Ali S., Ullah Khan S., Althobaiti S., Khan I., Alqurashi F., Kchaou M., Influence of variable fluid properties on mixed convective Darcy–Forchheimer flow relation over a surface with Soret and Dufour spectacle. Open Physics, 22(1), 20240010 (2024).

[20] Pamuk M.T., Numerical Simulation of Pressure Loss in Porous Media in Oscillating Flow, *WSEAS Transactions on Fluid Mechanics, 13, pp. 37-44, (2018).*

[21] Salawu S. O., Analysis of Third-Grade Heat Absorption Hydromagnetic Exothermic Chemical Reactive Flow in a Darcy-Forchheimer Porous Medium with Convective Cooling, *WSEAS Transactions on mathematics, 17, 280-289, (2018).*

[22] Tsuji K., Fujioka S., Morikawa D.S. et al. A reliable SPH(2) formulation for

Darcy–Forchheimer–Brinkman equation using a density-based particle shifting in the ALE description. Comp. Part. Mech. (2024).

[23] Zhang W. and Mehrabian A., Nonlinear and non-local analytical solution for Darcy–Forchheimer flow through a deformable porous inclusion within a semi-infinite elastic medium, *Journal of Fluid Mechanics, 911, (2021).*

[24] Fabrie P., Regularity of the solution of Darcy-Forchheimer's equation. *Nonlinear Anal. Theory Methods, 13, 1025-1045, (1989).*

[25] Ciarlet P. G., Basic error estimates for elliptic problems,*In Handbook of Numerical Analysis, Vol. II, Handbook of Numerical Analysis, pages 17-351. North-Holland, Amsterdam, (1991).*

[26] Dib S., Girault V., Hecht F. and Sayah T., A posteriori error estimates for Darcy'a problem coupled with the heat equation, *ESAIM: M2AN (53), 2121-2159, (2019).*

[27] Raviart P.-A., Thomas J.M., A mixed finite element method for 2-nd order elliptic problems, *Mathematical Aspects of the Finite Element Method. Lecture Notes in Mathematics, vol. 606, 292-315, Springer, Berlin (1977).*

[28] Brezzi, F., Douglas, J. Jr., Marini, L.D., Two families of mixed finite elements for second order elliptic problems, *Numer. Math. 47(2), 217-235 (1985).*

[29] Hecht F., New development in FreeFem++, *Journal of Numerical Mathematics, 20, 251–266, (2012).*

Contribution of Individual Authors to the Creation of a Scientific Article (Ghostwriting Policy)

The authors equally contributed in the present research, at all stages from the formulation of the problem to the final findings and solution.

Sources of Funding for Research Presented in a Scientific Article or Scientific Article Itself

No funding was received for conducting this study.

Conflict of Interest

The authors have no conflicts of interest to declare that are relevant to the content of this article.